Applied Surface Science 547 (2021) 149109

Contents lists available at ScienceDirect

Applied Surface Science

journal homepage: www.elsevier.com/locate/apsusc

Optical and electrical properties of amorphous alloy metal mesh for transparent flexible electrodes

Eun-Soo Park [a], Dae-Young Kim [b], Ju-Ho Lee [a], Jong-Uk Hwang [a], Ye-Seul Song [c], Keum-Hwan Park [c], Hyun-Joo Choi [b,*]

[a] Research and Development Center, Eloi Materials Lab (EML) Co. Ltd., Suwon 16229, Republic of Korea
[b] Department of Advanced Materials Engineering, Kookmin University, Seoul 02707, Republic of Korea
[c] Display Research Center, Korea Electronics Technology Institute, Sung-Nam 13509, Republic of Korea

ARTICLE INFO

Keywords:
Amorphous alloy thin film (ATF)
Flexible
Metal mesh
Aluminum
Rare earth
Transparent electrode

ABSTRACT

Amorphous alloy thin films are promising materials for next-generation flexible electrode applications because of their large elastic strain limit, high strength, and high oxidation resistance. Here, we propose an Al-based amorphous thin film as a new transparent electrode material that exhibits excellent optical and electrical properties as well as bending durability. Furthermore, the good heat and corrosion resistivity of these Al-based amorphous thin films makes them extremely promising as next-generation flexible transparent electrodes used under various environment.

1. Introduction

Transparent conducting electrodes (TCEs) are crucial components for various optoelectronic devices that require transport of both electrons and photons, including light emitting diodes (LEDs), touch screens, and solar cells [1]. The most commonly used TCE, indium tin oxide (ITO), provides high transparency and low sheet resistance simultaneously [2]. However, its brittle nature [3] and high processing cost [4] have limited commercialization of ITO electrodes.

Recently, carbon nanotubes (CNTs) [5–7], graphene [7], conductive polymers [8], metal nanowires [7], and metal mesh structures [9,10] have shown certain promising properties for transparent conducting electrodes. However, the performance of nano-carbon materials or conductive polymers is limited by their moderate sheet resistance, although they provide excellent flexibility [5,6,8]. Although silver nanowire networks exhibit low fabrication costs, high conductivity, transparency, and flexibility, they suffer from several problems such as the difficulty in developing a uniform nanowire distribution on a substrate, significant roughness of the networks, inferior electrical contact between the nanowires, and delamination of the nanowires from a substrate [7]. Metal mesh electrodes are a promising alternative because both their sheet resistance and optical transmittance are easily controlled by varying the grid width, spacing, and thickness, they exhibit a reduced junction resistance, and the work function of the electrode can be easily tuned by changing the metallic materials [9–10]. However, metal mesh electrodes lack the flexibility required for flexible electronics and repetitive plastic deformation increases sheet resistance. For flexible electronic applications, new material are required with high elastic strain limits and low electrical resistance. Amorphous alloys are a new class of metallic alloys with a unique amorphous atomic structure that results in a large elastic strain limit, high strength, and oxidation resistance [11,12].

Here, we propose Al-based amorphous alloys as a new transparent electrode material. Aluminum was selected as the base metal for better electrical conductivity and corrosion resistivity. Direct sputtering from a pre-alloyed single target enabled the formation of a fully amorphous structure of thin films despite the relatively low glass-forming ability of the Al-based alloys. The transmittance, sheet resistivity, bending durability, and heat and corrosion resistivity of amorphous thin films were investigated and compared with previously studied transparent electrodes

2. Materials and methods

Al-Y-Ni-Co thin films were deposited from an alloyed single target using a direct-current (DC) magnetron sputtering system. The sputter target was synthesized by hot isostatic pressure (HIP) of gas-atomized Al-Y-Ni-Co powder at 540 °C. Polyimide (PI) films used as elastomer

* Corresponding author.
E-mail address: hyunjoo@kookmin.ac.kr (H.-J. Choi).

https://doi.org/10.1016/j.apsusc.2021.149109
Received 15 October 2020; Received in revised form 11 January 2021; Accepted 19 January 2021
Available online 23 January 2021

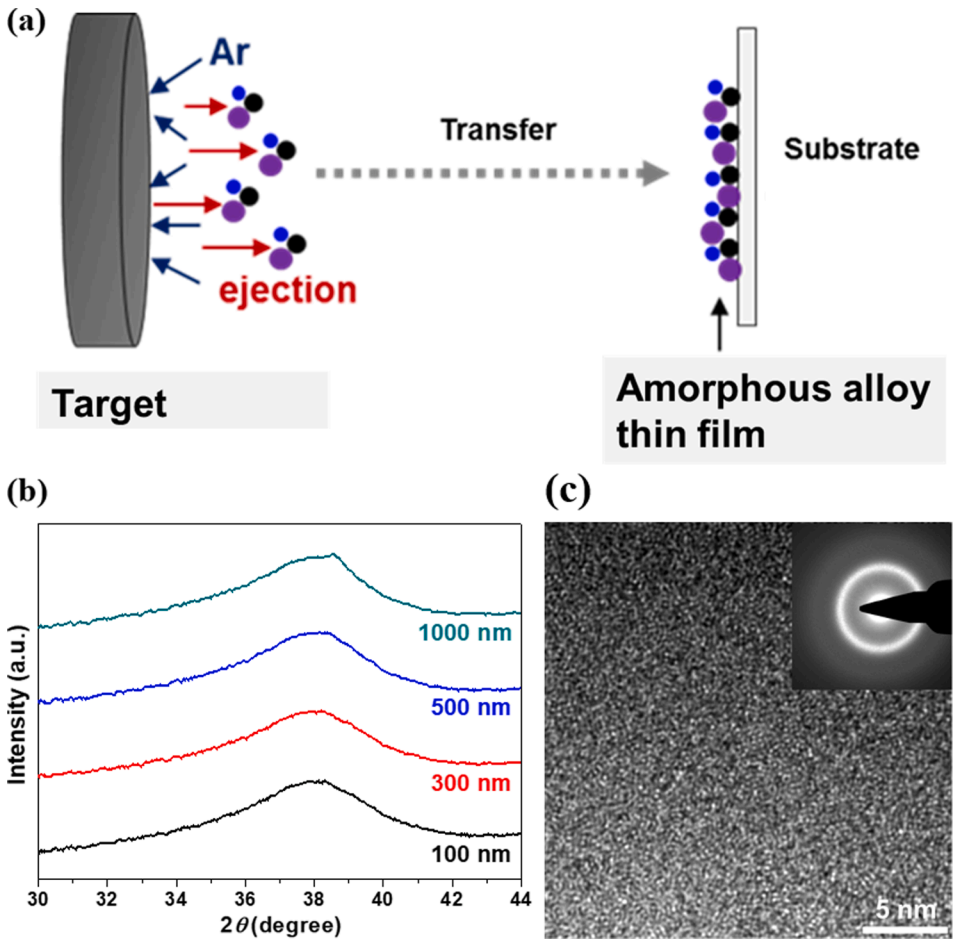

Fig. 1. (a) Schematic illustration of the atom transfer process during sputtering of Al-based amorphous alloy thin films. (b) XRD spectra of the thin film at various film thicknesses and (c) an HRTEM image and the corresponding diffraction pattern of the film (thickness: 100 nm).

substrates were ultrasonically cleaned with ethanol prior to deposition, and then placed inside the sputtering system at a base pressure of 1×10^{-6} Torr and sputter cleaned for 30 min using an O_2 plasma at 24 W and 2×10^{-2} Torr. Al-based amorphous films with thicknesses ranging from 10 to 1000 nm were deposited onto the PI elastomers. The sputtering process was performed below 333 K at a DC power of 200 W and a working gas Ar pressure of 5×10^{-3} Torr. The nominal target-substrate distance was 120 mm, and the deposition rate was approximately 25 nm/min.

Optically transparent electrodes were fabricated by photolithography processes. First, the films were spin-coated using a positive photoresist (PR) solution (GRX 601, a mixture of ethyl lactate, n-butyl acetate, diazonaphthoquinonesulfonic ester, and Cresol novolak resin, purchased from Merck) at 3000 rpm for 30 s under ambient conditions. After spin-coating, the samples were soft-baked at 100 °C for 2 min in air. A shadow mask, designed to produce patterns with a grating of 20 μm line width and 240 μm period, was aligned on the films. The PR was then exposed to 365 nm UV light (7 mW/cm^2) for 4 s (MA6, Karl Suss), developed in DPD 200 solution (containing Na and F particles, purchased from Dongjin Semichem) for about 1 min, and hard-baked at 120 °C for 5 min in N_2. After that, the PR was removed by etching with a typical aluminum etchant (mixture of 5% HNO_3, 75% H_3PO_4, 10% CH_3COOH, and 10% H_2O). Although PR was etched away after this process, acetone was also used to strip the remaining PR.

The amorphous structures of the as-deposited films were examined using X-ray diffraction (XRD, Brucker-AXS) with Cu Ka radiation (λ_{Cu} = 0.154187 nm) and high-resolution transmission electron microscopy (HRTEM). The optical transmittance of the patterned films was measured using a UV–VIS spectrophotometer (CM-3600d, Konica Minolta). The flexibility of the sputtered thin films was examined by R-bending tests at room temperature. The sheet resistance of the sputtered thin films was measured using four-probe techniques (MCP-T610, Mitsubishi Chemical) and at least 5 measurements were performed to verify the accuracy and scatter of the data. The heat resistance and corrosion resistance of the Al-Y-Ni-Co films were investigated by heating them at 250 °C for 30 min or by subjecting them to salt spray tests with a 5% sodium chloride solution injected at 1 bar pressure for 72 h, respectively. The same tests were repeated with silver films for reference.

3. Results and discussion

Fig. 1 (a) shows a schematic illustration of the atom transfer process during sputtering when using a pre-alloyed single target. Since all elemental atoms were pre-alloyed in the powder state, the target had good compositional uniformity at the atomic scale. Hence, alloy clusters can be simultaneously ejected from the alloyed target and deposited to the substrate during sputtering. This better stoichiometric transfer from the target to the film may prevent segregation of certain atoms or formation of unwanted inclusions in the films. For alloys with high glass-forming abilities (e.g., Zr-based or Cu-based alloys), an amorphous structure can be readily formed throughout thin films, although the chemical composition was not precisely controlled during sputtering because of different sticking coefficients and volatilities of elemental atoms [13]. For Al-based alloys with relatively low glass-forming ability, the bottleneck to deposit amorphous films can be overcome by using a single pre-alloyed target.

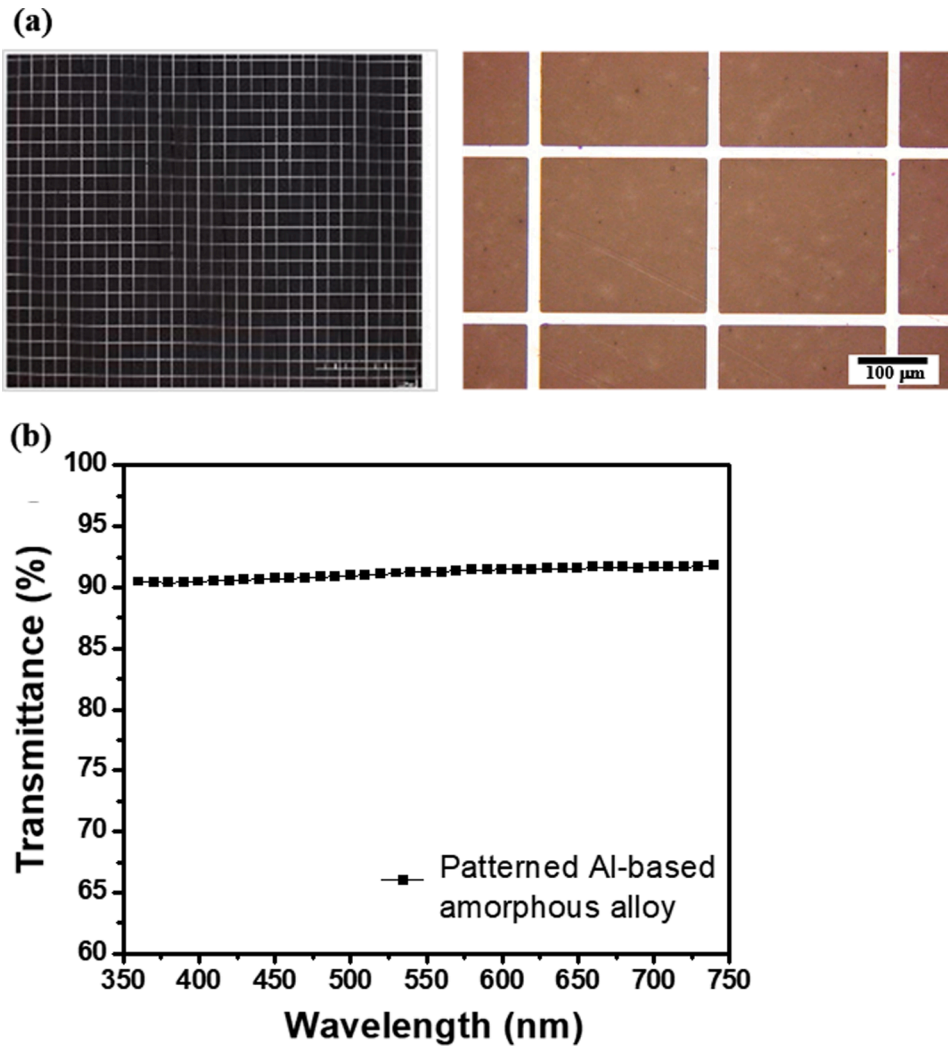

Fig. 2. (a) Optical images of the patterned Al-based amorphous alloy thin films and (b) transmittance spectra of the Al-based amorphous alloy thin films in the range of visible light wavelengths.

Fig. 1 (b) shows the XRD patterns of the films with various thicknesses. All the patterns exhibited a broad peak centered at 38°, typical of amorphous aluminum materials that have no long-range order regardless of the thickness of the films. This broad peak corresponds to the (1 1 1) plane of aluminum. Furthermore, the (1 1 1) peak slightly shifted to a higher value (closer to their ideal value) because the average atomic bonding length (Å) of the amorphous films decreased with increasing thickness of the films. The different thermal expansion behavior of the substrate and amorphous thin film as well as the average atomic bonding length mismatch may lead to the enlargement of the average atomic bonding length of the amorphous thin film near the substrate/thin film interface [14].

The amorphous structure of the deposited films was also confirmed by HRTEM observation and selected area diffraction (SAD) patterns collected from the corresponding area, as shown in Fig. 1 (c). No crystallites were observed in the image. Furthermore, a diffuse halo ring of the SAD pattern indicated a uniform amorphous microstructure without any crystalline features.

Fig. 2(a) shows an optical image of the patterned films. The actual line width was ~2 μm wider than that of the shadow mask (i.e., 18 μm) because of the shadowing effect [15]. Fig. 2 (b) shows the UV–Vis transmittance spectra of the patterned thin film (100 nm thickness), and the transmittance of the patterned film was greater than 90% throughout the visible range. The figure of merit (Φ) for evaluating the performance for transparent electrodes near 90% transparency is typically defined as $\Phi = T^{10}/R_s$, where T is the transmittance and R_s is the sheet resistance. At 550 nm, the figure of merit was calculated as $7.1 \times 10^{-3}\ \Omega^{-1}$ for the 100 nm-thick film, which is much higher than that of the Pt-coated nanowire electrodes ($2.8 \times 10^{-3}\ \Omega^{-1}$), ITO electrodes ($1.5 \times 10^{-3}\ \Omega^{-1}$), Cu grid ($0.5 \times 10^{-3}\ \Omega^{-1}$), and graphene electrodes ($0.4 \times 10^{-3}\ \Omega^{-1}$) [16].

In addition to their good optical and electrical properties, it is likely that these Al-based amorphous thin films exhibited excellent mechanical flexibilities because of the good elastic deformation capability of metallic glasses. To investigate the mechanical flexibility of the sputtered films, R-bending tests were conducted using rods with 1.5–10.5 mm at room temperature, as depicted as t_2 in the inset of Fig. 3 (a). In Fig. 3 (a), Al-based amorphous films as thin as 3 μm withstood 180° mechanical bending for 50,000 cycles without significant changes in sheet resistance. Notably, the original resistance can be almost restored, even for a bending radius of 1.5 mm, exhibiting extreme mechanical stability in comparison with conventional materials used in flexible electronics [17]. Fig. 3 (b) shows the change in the sheet resistance of the Al-based amorphous alloy and crystalline Al thin films as a function of the number of bending cycles using 1.5 mm diameter rods. The sheet resistance values of Al-based amorphous thin films remained extremely low, even after 5×10^4bending cycles, while those for crystalline Al significantly increased after 1×10^4bending cycles.

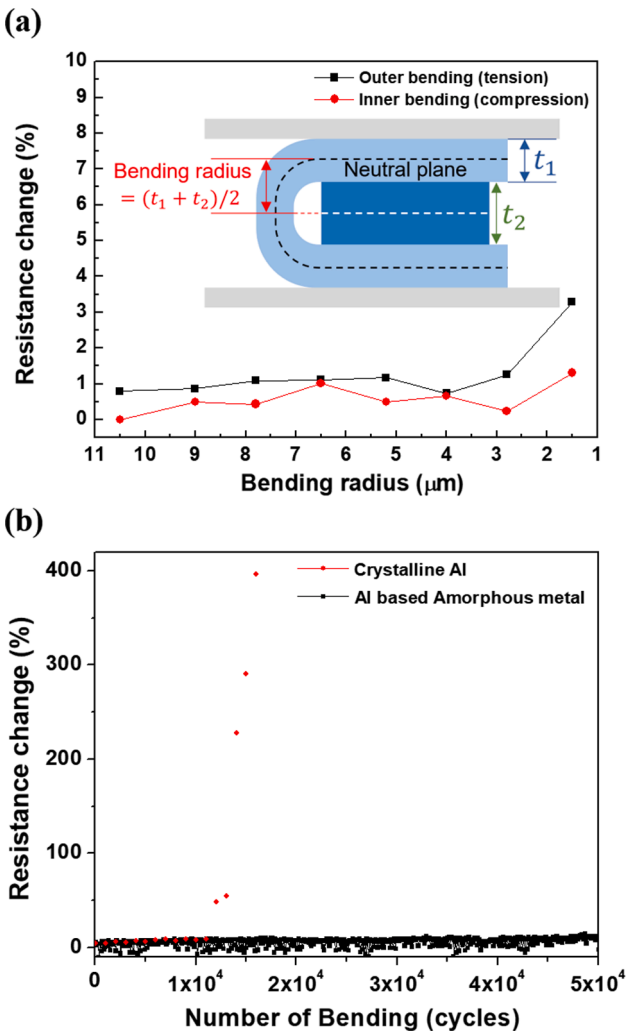

Fig. 3. Change of sheet resistance of (a) Al-based amorphous alloy measured in the outer and inner bending areas after bending tests at various bending radii and (b) data obtained from Al-based amorphous alloy and crystalline Al thin films as a function of number of bending cycles.

The heat resistance and corrosion resistance of the Al-Y-Ni-Co films were compared with those of the Ag thin films. After heating at 250 °C for 30 min, the Al-based amorphous thin film did not exhibit a notable change, while the Ag thin film was significantly oxidized as shown in Fig. 4 (a). Furthermore, the sheet resistance did not change significantly when an amorphous film was deposited. After salt spray tests with 5% sodium chloride, Al-based amorphous films also exhibited negligible change as shown in Fig. 4 (b), while the Ag film was significantly oxidized, leading to a notable increase in sheet resistance.

4. Conclusions

We have demonstrated super-elastic Al-based amorphous meshes as a new transparent electrode material. This amorphous thin film mesh exhibited great mechanical flexibility as well as excellent optical and electrical properties as a transparent electrode; the figure of merit of the amorphous thin film was ~2.5 times higher than that of Pt nanowire electrodes. Furthermore, the amorphous thin film exhibited far better heat and corrosion resistivity than the thin silver film because of its high resistance against oxidation.

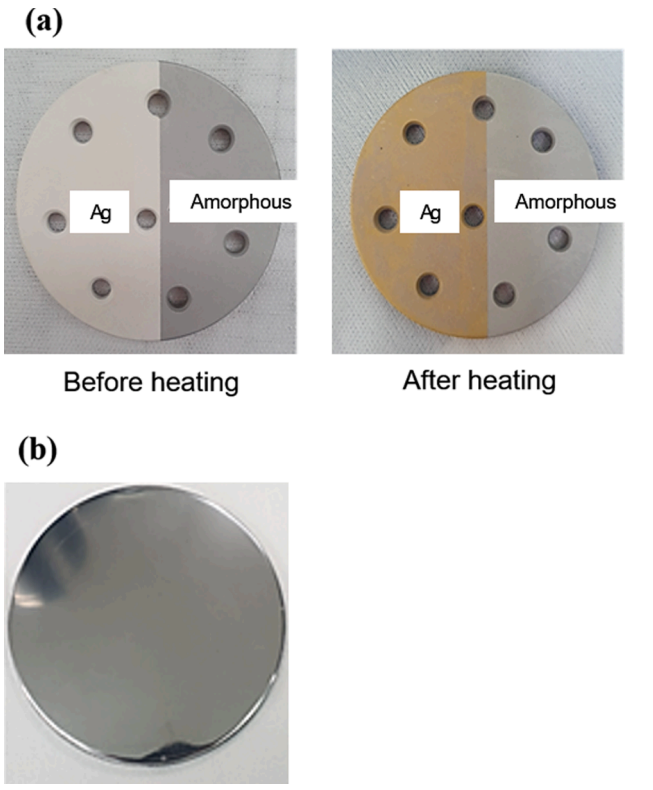

Fig. 4. (a) Comparison of optical images of Ag and Al-based amorphous alloy thin films before and after heating at 250 ℃ for 30 min in air. (b) An optical image of the Al-based amorphous alloy thin film wafer after salt spray test for 72 h.

CRediT authorship contribution statement

Eun-Soo Park: Conceptualization, Supervision. **Dae-Young Kim:** Data curation, Writing - review & editing. **Ju-Ho Lee:** Data curation. **Jong-Uk Hwang:** Methodology. **Ye-Seul Song:** Investigation. **Keum-Hwan Park:** Writing - review & editing. **Hyun-Joo Choi:** Writing - original draft, Supervision, Data curation.

Declaration of Competing Interest

The authors declare that they have no known competing financial interests or personal relationships that could have appeared to influence the work reported in this paper.

Acknowledgements

This work was supported by the National Research Foundation of Korea(NRF) grant funded by the Korea government(MSIT) (No. 2020R1A2C2101047).

References

[1] D.S. Hecht, L. Hu, G. Irvin, Emerging transparent electrodes based on thin films of carbon nanotubes, graphene, and metallic nanostructures, Adv. Mater. 23 (13) (2011) 1482–1513, https://doi.org/10.1002/adma.201003188.
[2] R.G. Gordon, Criteria for choosing transparent conductors, MRS Bull. 25 (8) (2000) 52–57, https://doi.org/10.1557/mrs2000.151.
[3] C. Peng, Z. Jia, D. Bianculli, T. Li, J. Lou, In situ electro-mechanical experiments and mechanics modeling of tensile cracking in indium tin oxide thin films on polyimide substrates, J. Appl. Phys. 109 (10) (2011) 103530, https://doi.org/10.1063/1.3592341.
[4] N.-R. Kim, J.-H. Lee, Y.-Y. Lee, D.-H. Nam, H.-W. Yeon, S.-Y. Lee, T.-Y. Yang, Y.-J. Lee, A. Chu, K.T. Nam, Y.-C. Joo, Enhanced conductivity of solution-processed indium tin oxide nanoparticle films by oxygen partial pressure controlled

annealing, J. Mater. Chem. 1 (37) (2013) 5953, https://doi.org/10.1039/c3tc31037j.
[5] Z. Yu, L. Hu, Z. Liu, M. Sun, M. Wang, G. Gruner, Q. Pei, Fully bendable polymer light emitting devices with carbon nanotubes as cathode and anode, Appl. Phys. Lett. 95 (2009) 2033–2037, https://doi.org/10.1063/1.3266869.
[6] P.N. Nirmalraj, P.E. Lyons, S. De, J.N. Coleman, J.J. Boland, Electrical connectivity in single-walled carbon nanotube networks, Nano Lett. 9 (11) (2009) 3890–3895, https://doi.org/10.1021/nl9020914.
[7] S. De, J.N. Coleman, Solution-processed transparent electrodes: The effects of percolation in nanostructured transparent conductors, MRS Bull. 36 (10) (2011) 774–781, https://doi.org/10.1557/mrs.2011.236.
[8] M. Vosgueritchian, D.J. Lipomi, Z. Bao, Highly conductive and transparent PEDOT:PSS films with a fluorosurfactant for stretchable and flexible transparent electrodes, Adv. Funct. Mater. 22 (2) (2012) 421–428, https://doi.org/10.1002/adfm.201101775.
[9] X. Ho, H. Lu, W. Liu, J.N. Tey, C.K. Cheng, E. Kok, J. Wei, Electrical and optical properties of hybrid transparent electrodes that use metal grids and graphene films, J. Mater. Res. 28 (4) (2013) 620–626, https://doi.org/10.1557/jmr.2012.399.
[10] K.o. Higashitani, C.E. McNamee, M. Nakayama, Formation of large-scale flexible transparent conductive films using evaporative migration characteristics of Au nanoparticles, Langmuir 27 (6) (2011) 2080–2083, https://doi.org/10.1021/la103902z.
[11] M.M. Trexler, N.N. Thadhani, Mechanical properties of bulk metallic glasses, Prog. Mater. Sci. 55 (8) (2010) 759–839, https://doi.org/10.1016/j.pmatsci.2010.04.002.
[12] J. Schroers, J. Bulk Metallic Glasses, Phys. Today 66 (2013) 32–37.
[13] Y.P. Deng, Y.F. Guan, J.D. Fowlkes, S.Q. Wen, F.X. Liu, G.M. Pharr, P.K. Liaw, C. T. Liu, P.D. Rack, A combinatorial thin film sputtering approach for synthesizing and characterizing ternary ZrCuAl metallic glasses, Intermetallics 15 (9) (2007) 1208–1216, https://doi.org/10.1016/j.intermet.2007.02.011.
[14] G.H. Jo, S.-H. Kim, J.-H. Koh, Enhanced electrical and optical properties based on stress reduced graded structure of Al-doped ZnO thin films, Ceram. Int. 44 (1) (2018) 735–741, https://doi.org/10.1016/j.ceramint.2017.09.240.
[15] V. Kostianovskii, B. Sanyoto, Y.Y. Noh, A facile way to pattern PEDOT:PSS film as an electrode for organic devices, Org. Electron. 44 (2017) 99–105, https://doi.org/10.1016/j.orgel.2017.02.007.
[16] Y. Yang, L. Wang, H. Yan, S. Jin, T.J. Marks, S. Li, Highly transparent and conductive double-layer oxide thin films as anodes for organic light-emitting diodes, Appl. Phys. Lett. 89 (5) (2006) 051116, https://doi.org/10.1063/1.2240110.
[17] K.S. Kim, Y. Zhao, H. Jang, S.Y. Lee, J.M. Kim, K.S. Kim, J.-H. Ahn, P. Kim, J.-Y. Choi, B.H. Hong, Large-scale pattern growth of graphene films for stretchable transparent electrodes, Nature 457 (7230) (2009) 706–710, https://doi.org/10.1038/nature07719.